

A method for the determination of infrared optical constants from reflectance measurements on powdered samples

This article has been downloaded from IOPscience. Please scroll down to see the full text article.

1994 J. Phys.: Condens. Matter 6 7125

(<http://iopscience.iop.org/0953-8984/6/35/021>)

View [the table of contents for this issue](#), or go to the [journal homepage](#) for more

Download details:

IP Address: 171.66.16.151

The article was downloaded on 12/05/2010 at 20:26

Please note that [terms and conditions apply](#).

A method for the determination of infrared optical constants from reflectance measurements on powdered samples

Carlos Pecharromán and Juan E Iglesias

Instituto de Ciencia de Materiales, Consejo Superior de Investigaciones Científicas, Calle Serrano, 115 duplicado, Madrid 28006, Spain

Received 5 April 1994, in final form 5 May 1994

Abstract. A method for determining the infrared dielectric constant function of an isotropic material from measurement of the reflectance from powdered samples has been implemented. The method is based on an expression for the average dielectric constant of a heterogeneous system, which shows percolation features. The results obtained through the use of this method compare well with published results from single-crystal reflectance data, and show that damping factors in powders are moderately higher than those measured for single crystals. The method works best if samples are made of small microparticles (less than $2\ \mu\text{m}$), pressed to filling factors less than 0.6. Some precaution should be exercised with plastic ionic substances. The method can be used to determine the dielectric constant of a large number of compounds that cannot be obtained as centimetre-sized single crystals.

1. Introduction

The determination of the complex dielectric function in the infrared (IR) as a function of wavenumber has been widely employed in the last 30 years in solid state physics [1–3] to provide important information about optical phonons in the $k = 0$ region. This dielectric function, sometimes loosely referred to as ‘dielectric constant’, is customarily obtained from the measured reflectance spectrum of the material, but, to date, this technique has been restricted to substances that could be grown as centimetre-sized single crystals. Since most solid chemical compounds are polycrystalline when synthesized (or found in Nature), the extension of this method of measurement to powdered samples would be a worthwhile objective. Some attempts have indeed been made in the past few years [4–6] to extract this kind of information from pressed powders or polished rock samples. These relied on simple models in which the pellet reflectance was corrected by dividing it by the volume ratio of the particles in the pressed pellet [6] or else by applying a similar correction to the dielectric constant obtained through Kramers–Kronig transformation [5]. However, more detailed studies [7] have shown that these direct corrections are grossly inadequate and that unsophisticated methods must be discarded. Some tests performed by us in which IR absorption spectra of diluted Co_3O_4 particles were fitted using dielectric constants obtained from pressed powder pellets [6] have shown significant lack of agreement between experimental and calculated spectra.

Because direct corrections fail to give an adequate solution, it appears that a more appropriate way to approach this problem should begin with a deeper knowledge of the behaviour of the dielectric constant of pressed pellets. A correct description of such behaviour can be obtained from some of the various theories of the average dielectric constant for heterogeneous systems. Several different formulations [8–11] exist, each

appropriate for different ranges of filling factor or dielectric constant of the system components. The oldest and best known is that of Maxwell-Garnett [12] (MGT), but formulations by Bruggemann [13] and Landauer [14, 15], called effective-medium theory (EMT), have enjoyed a comparable degree of popularity. From these original works, three different methodologies to deal with the average dielectric constant have emerged. The MGT, an asymmetric formulation because one has to make a choice as to which component is 'particle' and which is 'matrix', has proved to be accurate in the calculation of IR dielectric constants for diluted heterogeneous aggregates [8, 16–21]. Bruggemann's expression [13] introduces a differential procedure to calculate the average electrical conductivity (the formalism for the dielectric constant is exactly the same) for heterogeneous mixtures, which has shown itself to be a very useful theoretical tool for describing the mathematical properties of average dielectric constant theories [22–24], and it is the natural way to describe dielectric properties of fractal and self-similar materials [25]. Together with this differential approach, Bruggemann subsequently made use of the so-called EMT principle, which assumes that the field around each particle (matrix and inclusions are treated symmetrically in EMT) immersed in the heterogeneous system is a constant. Finally, Landauer's EMT formulation [14, 15] has been widely used to explain conductivity and dielectric constant properties [9–11] of particle mixtures. Recently, the present authors [26] have developed a new approach by combining the EMT principle with the fact, suggested by numerical simulation, that percolation features must be taken into consideration in the computation of the dielectric constant in heterogeneous systems. We use these previous results to link in this work the average optical properties of the pressed pellet with the dielectric constant of the microparticles, and show that this approach can be used to determine the optical parameters in the infrared of inorganic materials when macroscopic crystals are unavailable. Like most average dielectric theories, ours is formulated for static fields; it is clear that at IR frequencies, the condition that the wavelength be larger than the particle size is easily satisfied for colloidal sized particles, so, in a first approximation, retardation effects can be neglected and static-field EMT can be used for these particles.

2. Experimental details

Measurements of the IR reflectance at near to normal incidence have been made on pressed pellets composed of very small spherical or cubical particles of NiO, MgO, MgAl₂O₄, CaF₂ and SrTiO₃ (figure 1). The NiO, CaF₂ and MgO samples were obtained from commercial sources, and were subject to annealing at 400 °C for 5 h, prior to reflectance measurements. These samples were composed of small (0.2 μm average diameter) rounded particles. The MgAl₂O₄ and SrTiO₃ samples, consisting of small spheres 0.1–0.4 μm in diameter, were synthesized by a procedure of spray pyrolysis [27] and subsequently heated at a temperature of 1050 °C for spinel and 850 °C for strontium titanate to improve the crystallinity. Whilst the spinel particles preserved their spherical shape (figure 1(d)), the particles of strontium titanate took on a cubic-like aspect (figure 1(g)). All the samples were characterized by x-ray diffraction (XRD), transmission electron microscopy (TEM) and/or scanning electron microscopy (SEM) and transmission IR spectroscopy.

For the specimens required for reflectance measurements, the powders were compressed in a vacuum under 800 MPa with a very smooth die made of YSZ (yttria-stabilized zirconia). The resulting pellets had a high-quality reflecting surface, with very low values of the roughness coefficient for IR optics (around 0.5–0.3 μm) [28, 29]. Absorbance samples were the usual KBr pellets.

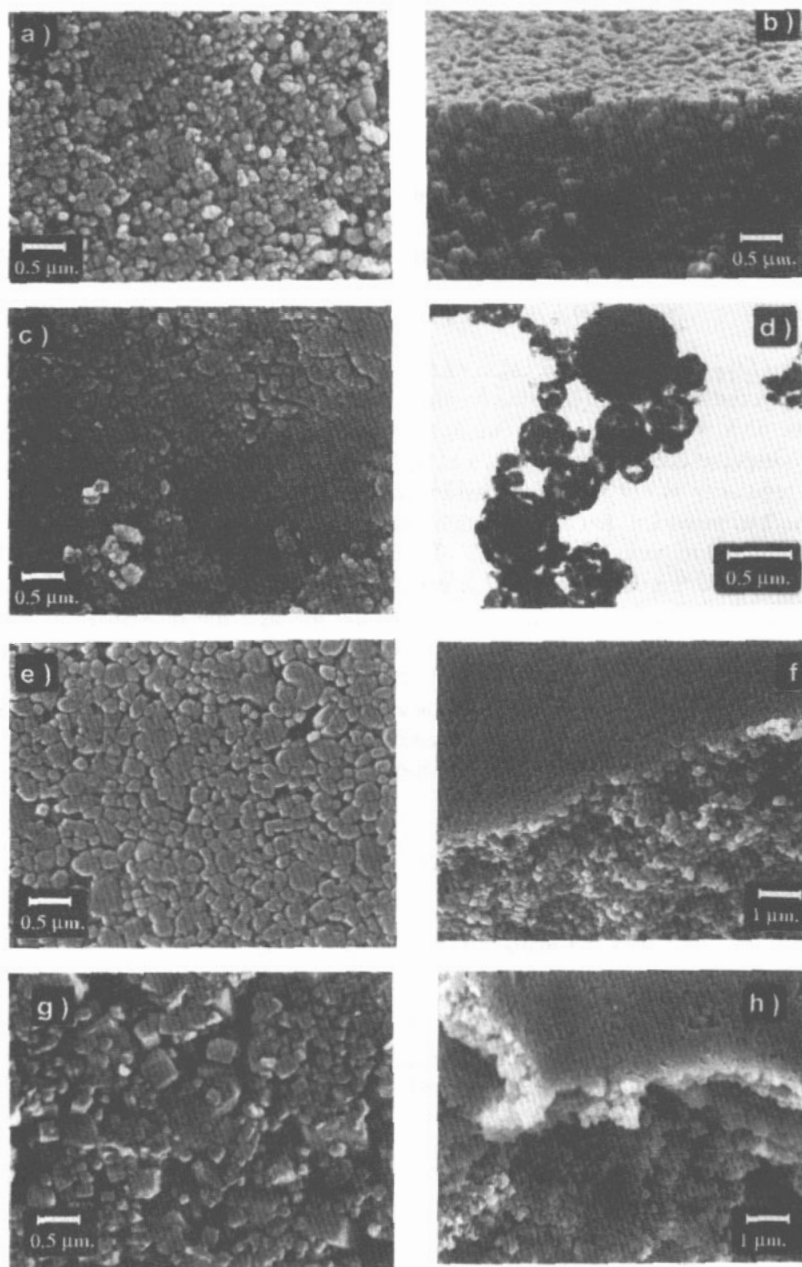


Figure 1. Transmission (*d*) and scanning (other) electron micrographs of the materials used in this work: (*a*) NiO, pellet surface. (*b*) NiO, pellet broken edge showing smooth surface and jagged side. (*c*) MgO, pellet surface, showing some degree of recrystallization. (*d*) Spinel, MgAl₂O₄, spherical particles seen in transmission. (*e*) CaF₂, pellet surface; pressure recrystallization is noticeable. (*f*) CaF₂, smooth surface and jagged side of broken pellet. (*g*) SrTiO₃, cube-shaped crystallites. (*h*) SrTiO₃, pellet surface showing signs of pressure sintering, and side.

The IR specular reflectance spectra were measured with a Nicolet 20 SXC and a Nicolet 20 F FTIR spectrophotometer in the range of 3950–210 cm^{-1} and 600–100 cm^{-1} respectively, sampling every 0.48 cm^{-1} . Absorbance was measured in the Nicolet 20 SXC spectrometer, at a resolution of 2 cm^{-1} .

3. Theory and computational methods

The average dielectric constant of a particle aggregate can be defined by

$$\langle \epsilon \rangle = \langle D \rangle_{E_0} / \epsilon_0 \langle E \rangle_{E_0} \quad (1)$$

where $\langle D \rangle_{E_0}$ is the average value of the displacement parallel to the external applied field, $\langle E \rangle_{E_0}$ is the same average value for the electric field and ϵ_0 is the permittivity of free space.

In this work, we have studied systems composed of air- and pressure-packed monodisperse colloidal particles, i.e. particles having all the same shape and size; perfect size regularity is not strictly necessary, and the formulae we use do not contain size as a parameter, provided that it is less than the wavelength, as mentioned above. Our equations are restricted to particles having the shape of ellipsoids of revolution (spheroids), coming in two varieties, 'particles', for which we use subscript p, and 'matrix', denoted by subscript m. Shape is incorporated into the equations through the depolarization factors L_p and L_m corresponding to the direction normal to the revolution axis of the spheroids; these are functions of r , the axial ratio of the spheroids. Both particle and matrix materials are considered isotropic in what follows, with dielectric constants denoted by ϵ_m and ϵ_p , although anisotropic cases can be treated under favourable circumstances. Under these conditions, the average dielectric constant can be calculated by

$$\left(\frac{2(1-f)(\langle \epsilon \rangle - \epsilon_m)}{(1-L_m)\langle \epsilon \rangle + L_m\epsilon_m} + \frac{(1-f)(\langle \epsilon \rangle - \epsilon_m)}{2L_m\langle \epsilon \rangle + (1-2L_m)\epsilon_m} \right) + \left(\frac{2f(\langle \epsilon \rangle - \epsilon_p)}{(1-L_p)\langle \epsilon \rangle + L_p\epsilon_p} + \frac{f(\langle \epsilon \rangle - \epsilon_p)}{2L_p\langle \epsilon \rangle + (1-2L_p)\epsilon_p} \right) = 0 \quad (2)$$

where f , the filling factor, is the volume fraction of 'p' material.

A detailed analysis of equation (2) reveals [26] that, when ϵ_p tends to infinity, the function $\langle \epsilon \rangle(f)$ shows a discontinuity at a certain value of the filling factor, $f = f_c$; f_c can be interpreted as a percolation threshold, and it can be proved that its value is given by the following expression:

$$f_c = H/(H + G) \quad (3)$$

where

$$H = (3L_m + 1)/(2L_m - 2L_m^2) \quad (4)$$

and

$$G = (2 - 3L_p)/(L_p - 2L_p^2). \quad (5)$$

In a real pressed pellet, spheroidal 'p' particles are thought to be included in an air matrix. A hypothesis employed above is that voids between inclusions have an average

ellipsoidal shape described by the depolarization constant L_m . However, it is not easy to estimate the effective value of L_m . It is easier instead to obtain f_c by experimental measurements. To that end, we rewrite the average dielectric constant expression in terms of f_c instead of L_m :

$$L_m = \frac{f_c[(3 + 2G) - 3] \pm \{f_c^2[(3 + 2G) - 3]^2 - 8Gf_c(1 - f_c)\}^{1/2}}{4Gf_c}. \quad (6)$$

The choice of sign in the above equation should be made in such a way that $0 < L_m < 1/2$; in most practical the cases the minus sign should be chosen. Using this expression, we can calculate $\langle \epsilon \rangle$ as a function of several variables:

$$\langle \epsilon \rangle = \langle \epsilon \rangle(\epsilon_p, \epsilon_m, L_p, f, f_c). \quad (7)$$

Our purpose is to estimate ϵ_p from measured data of the specular reflectance, $R(\omega)$, which can be related to $\langle \epsilon \rangle(\omega)$ through the Kramers-Kronig and Fresnel relations. Hence an inverse expression of equation (2) is required in order to calculate ϵ_p :

$$[\mathcal{H}(L_p - 2L_p^2) + (3L_p - 2)]\epsilon_p^2 + [\mathcal{H}(4L_p^2 - 3L_p + 1) + (1 - 6L_p)]\langle \epsilon \rangle\epsilon_p + [\mathcal{H}(2L_p - 2L_p^2) + (1 + 3L_p)]\langle \epsilon \rangle^2 = 0 \quad (8)$$

where

$$\mathcal{H} = \frac{(1 - f)}{f} \left(\frac{2(\langle \epsilon \rangle - \epsilon_m)}{(1 - L_m)\langle \epsilon \rangle + L_m\epsilon_m} + \frac{(\langle \epsilon \rangle - \epsilon_m)}{(2L_m)\langle \epsilon \rangle + (1 - 2L_m)\epsilon_m} \right) \quad (9)$$

However, although this method is useful to obtain a first approximation for ϵ_p , our data indicate that this procedure introduces errors, specially in the spectral region where $\text{Re}[\langle \epsilon \rangle(\omega)] \simeq 0$, where one frequently obtains negative values of $\text{Im}(\epsilon_p)$. For this reason, a least-squares procedure is employed in order to refine ϵ_p by direct comparison with the experimental reflectance data. For this purpose, classical (equation (10)) or semiquantum (equation (11)) [30, 31] models of superposition of oscillators have been assumed for ϵ_p :

$$\epsilon_p = \epsilon_\infty + \sum_{k=1}^N \frac{4\pi\rho_k\omega_{Tk}^2}{(\omega_{Tk}^2 - \omega^2) - i\gamma_k\omega} \quad (10)$$

$$\epsilon_p = \epsilon_\infty \prod_{k=1}^N \frac{\omega_{Lk}^2 - \omega^2 - i\gamma_{Lk}\omega}{\omega_{Tk}^2 - \omega^2 - i\gamma_{Tk}\omega} \quad (11)$$

Using the well known relationship between the dielectric constant and the reflectance:

$$R = [(\sqrt{\langle \epsilon \rangle} - 1)/(\sqrt{\langle \epsilon \rangle} + 1)]^2 \quad (12)$$

we perform a non-linear least-squares adjustment with M ($\simeq 1000$) experimental reflectance data to minimize the squared error function defined by

$$\Delta = \sum_{l=1}^M \{R_{\text{exp}}(\omega_l) - R_{\text{theo}}[\langle \epsilon \rangle(f, f_c, L_p; \epsilon_p(\omega_l))]\}^2. \quad (13)$$

The index $\mathcal{R} = [\sum (R_{\text{theo}} - R_{\text{exp}})^2 / \sum R_{\text{exp}}^2]^{1/2}$ was used to assess the quality of each least-squares fit.

In equation (13) ϵ_p can be calculated by the classical (equation (10)) or quantum expression (equation (11)). In these expressions, ϵ_{∞} , ω_{Tk} , γ_k , ρ_k or ϵ_{∞} , ω_{Tk} , γ_{Tk} , ω_{Lk} , γ_{Lk} are the parameter sets that determine the dielectric constant of microparticles, and f , f_c , L_p are geometrical factors that only depend on the shape of particles and on the way they pack in the pellet. In the software developed by us, all of these parameters are adjustable.

For the calculation of a first approximation of f_c and ϵ_{∞} we have employed the IR transparency region of the reflectance spectrum (around 1500 to 4000 cm^{-1}). If the roughness of the pellet surface is low and can be neglected, or else it has been adequately allowed for [28, 29], the reflectance in this region only depends on f , f_c and ϵ_{∞} . It should be pointed out, however, that f , f_c and ϵ_{∞} are parameters that present large values of the correlation coefficients, especially in the transparency region, so they are difficult to refine simultaneously, and it is advisable to obtain at least two of them from external sources, so their values can be fixed in the least-squares refinement. The first variable, f , can be obtained directly from measurement of the density of the pellet. The high-frequency dielectric constant ϵ_{∞} is in many cases available in the literature or else it can be measured by some other optical method; in this circumstance, f_c can be easily estimated and refined. If ϵ_{∞} were unknown, f_c can be taken as $f_c \simeq 0.9f$, as a starting approximation; this hypothesis is supported by the results of numerical simulations [26, 32]. Then we can use the least-squares procedure in the transparency region of the reflectance spectrum to compute ϵ_{∞} and f_c simultaneously. Our experience indicates that this simultaneous refinement gives final values of ϵ_{∞} having about a 10% error. Consequently we have preferred in the examples presented below to take ϵ_{∞} from the literature whenever it was available; we have however carried out a complete computation of all variables except f for the case of NiO, to show that the method can give a realistic estimation of all relevant optical parameters.

As soon as we have a first approximation of f , f_c and ϵ_{∞} , the estimation of the oscillator parameters is possible. The correct way to do it is to calculate the function $\langle \epsilon(\omega) \rangle$ in the *reststrahl* region by using the Kramers–Kronig relationships to obtain the phase of the reflectance. Equations (8) and (9) connect $\langle \epsilon(\omega) \rangle$ with $\epsilon_p(\omega)$. With this first estimate of $\epsilon_p(\omega)$ it is easy to determine approximate values of ϵ_{∞} , ω_{Tk} , γ_k , ρ_k or ϵ_{∞} , ω_{Tk} , γ_{Tk} , ω_{Lk} , γ_{Lk} . These values and the starting values of f , f_c and L_p (this can be obtained from the observed shape of the particles) are used to carry out the final non-linear least-squares computation over the whole measured reflectance spectrum.

We want to add some words about the experimental method of pellet preparation. The importance of obtaining pressed powder pellets with a high-quality specular surface cannot be overemphasized. If a pellet surface is rough, its reflectance spectrum suffers a strong distortion, especially in the high-frequency region, and the reflectance decreases with wavenumber instead of remaining constant, as would occur in this region for a smooth insulator surface; this, in turn, introduces a strong error in the high-frequency dielectric constant as calculated by the Kramers–Kronig transformations. For a well pressed powder pellet, the particle size gives the scale of surface roughness; it follows that only the use of microparticles of size equal to or less than 1 μm could satisfy the low-roughness condition in the infrared. Furthermore, these particles must be perfectly packed under a high pressure with a hard and very smooth striking surface. Our best results have been achieved through the use of a tough and hard YSZ (yttria-stabilized zirconia) ceramic die.

4. Results and discussion

We have carried out complete determinations of optical parameters by least-squares adjustments, as described in the previous section, from the measured reflectance spectra of the following compounds: NiO, MgO, MgAl₂O₄, CaF₂ and SrTiO₃. These materials were chosen because all of them are optically isotropic and can be easily obtained as microscopic monodisperse particles. The experimental spectra and best fit obtained are shown in figures 2–6 and the parameters corresponding to these results are in tables 1–5.

4.1. NiO

This substance crystallizes in space group $R\bar{3}m$ and its structure is a slight distortion of the $Fm\bar{3}m$ NaCl structure type. For this reason Gielisse *et al* [33] and Mochizuki and Satoh [34] considered this substance as optically isotropic in their determination of dielectric constants from the IR reflectance spectrum measured on a single crystal. Because there exist some differences between both sets of results, we have reproduced them, together with our results, in table 1.

Table 1. The IR optical parameters of NiO, from pressed powder pellet ($f = 0.53$, fixed) and a single crystal. Frequencies and damping factors in cm^{-1} .

	Powder		Single crystal	
	This paper (all parameters free)	This paper (ϵ_∞ fixed)	Ref. [33]	Ref. [34]
ω_{T1}	394.6 ± 0.4	395.3 ± 0.5	405	400
$4\pi\rho_1$	6.75 ± 0.04	6.62 ± 0.03	5.68	6.40
γ_1	14.1 ± 0.4	14.7 ± 0.4	18	11.04
ω_{T2}	560.2 ± 0.6	560.3 ± 0.8	560	563
$4\pi\rho_2$	0.13 ± 0.01	0.12 ± 0.01	0.37	0.126
γ_2	78 ± 3	75 ± 3	280	78.257
ϵ_∞	5.77	5.7 ^a	5.7 ^a	5.7 ^a
f_c	0.66	0.67	—	—
\mathcal{R}	0.03	0.03	—	—

^a Taken from [34].

We have chosen this substance as the main test of the fitting procedure. First we supposed that nothing was known on the NiO dielectric constant in the infrared. So, besides the measured value $f = 0.53$ we imposed $f_c = 0.5$. An initial value of $\epsilon_\infty = 5.6$ was obtained from the fit of the experimental reflectance spectrum in the transparency region. Then, a first estimate of the function ϵ_p was calculated from the spectrum $\langle\epsilon\rangle$ obtained from the reflectance spectrum by the use of the Kramers–Kronig and Fresnel relationships. This function was subsequently refined with the observed reflectance as the reference. The final fit appears in figure 2, and the refined values of the optical parameters are in table 1. A comparison between single-crystal data and our powder data reveals very good agreement between both kinds of data, for this simple two-phonon classical model; the agreement is particularly good between our powder data and the single-crystal data published by Mochizuki and Satoh [34], the difference being only a 5 cm^{-1} shift in ω_T to lower frequency, and practically negligible shifts in the values of the strength and damping factor of the oscillators. We carried out a second calculation in which we kept fixed $\epsilon_\infty = 5.7$, taken from the literature; the result, practically indistinguishable from the previous one, is also shown in table 1.

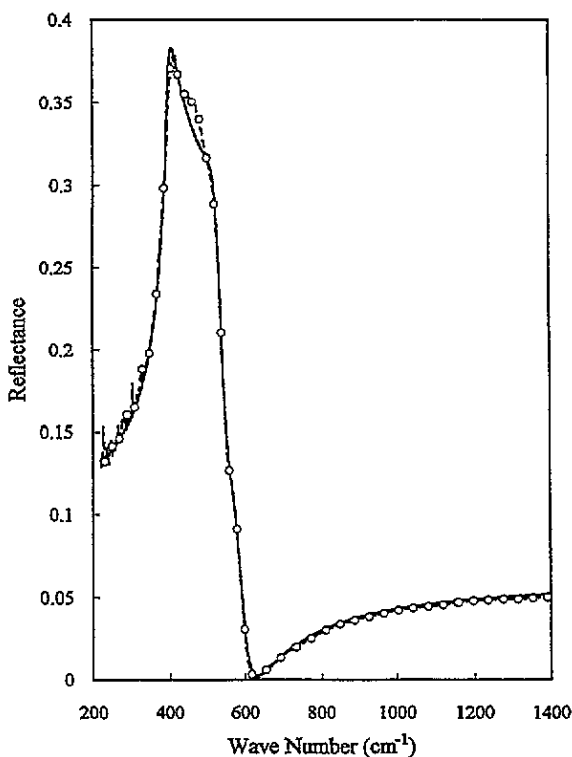


Figure 2. The IR reflectance spectrum of powdered NiO: (---○---) observed values; (—) values calculated with the parameters in first column of table 1.

4.2. MgO

The NaCl-type crystal structure of MgO belongs to space group $Fm\bar{3}m$ and hence is similar to that of NiO. The material has one main classical IR mode and a secondary oscillator [35]. However, a sharp maximum at 400 cm^{-1} appears in the powder reflectance spectrum, followed by two shoulders: the first one extends from 500 to 620 cm^{-1} , and then the reflectance decreases, featuring a second shoulder at 640 cm^{-1} (see figure 3). The band between 400 and 620 cm^{-1} corresponds to the main IR mode, and the 640 cm^{-1} shoulder can be readily identified as the secondary oscillator. Our calculation, based on $f = 0.56$, $\epsilon_{\infty} = 3.01$, reproduces well the maximum at 400 cm^{-1} and the shoulder at 640 cm^{-1} . However, the feature in the region between 500 and 620 cm^{-1} is not reproduced precisely by the theoretical spectrum, although the fit is at least qualitative; this behaviour in the reflectance spectra of particle aggregates is quite general (see the discussion in section 4.6). The oscillator parameters are in table 2, together with those published for a single crystal [35].

Comparison between the optical parameters deduced from single-crystal and powder reflectance reveals that both are very similar, except for the larger value of the damping parameter for the main oscillator in the case of the powder sample (9 cm^{-1} for powder versus 7.62 cm^{-1} for single crystal). There exists an abundance literature [8, 16, 21, 36, 37] on IR transmission spectra for MgO powder samples, containing theoretical calculations of such spectra, based on the absorption cross section or on MGT, which are compared with the experimental absorption spectra. In most of these works it is generally accepted that

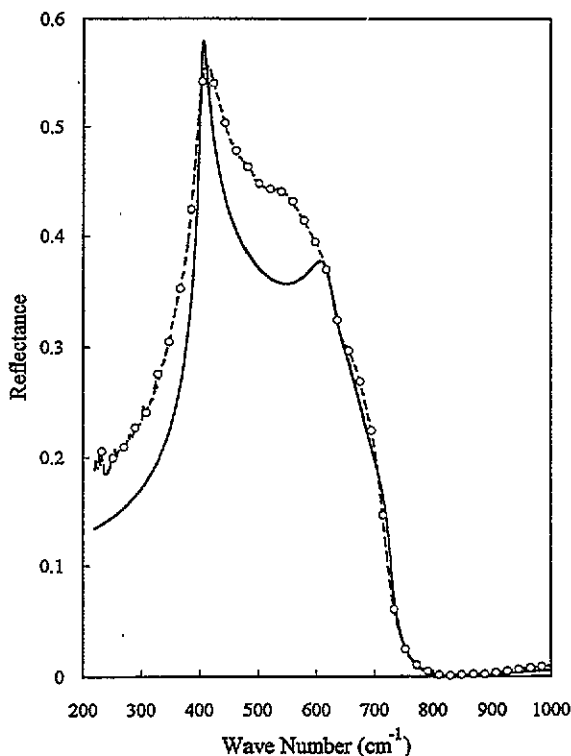


Figure 3. The IR reflectance spectrum of powdered MgO: (---○---) measured values; (—) values calculated with the PPP parameters in table 2.

Table 2. The IR optical parameters of MgO from pressed powder pellet ($f = 0.56$, $\epsilon_{\infty} = 3.01$ [35], fixed; $f_c = 0.5$, refined) obtained in this paper (PPP) by least-squares fit ($\mathcal{R} = 0.16$) compared with single-crystal (SC) parameters published by Jasperse *et al* [35].

ω_T (cm ⁻¹)		$4\pi\rho$		γ (cm ⁻¹)	
PPP	SC	PPP	SC	PPP	SC
405 ± 1	401	6.52 ± 0.07	6.62	9 ± 1	7.62
639 ± 6	640	0.03 ± 0.01	0.045	77 ± 17	102.4

the fit of experimental with calculated spectra in powdered samples requires the damping parameters to be from 2 to 10 times larger than those of a single crystal [16, 36]; however, some theoretical work [38, 39] predicts that the differences should not be so great, of the order of a factor of 2 for the worst cases. Our damping parameters corresponding to powdered MgO samples are only slightly higher (1.18 times) than those determined on a single crystal. We think that higher damping values found in the literature are due to some type of microparticle aggregation in the diluted samples used in transmission experiments. Moreover, if $f > 0.1$, the MGT and cross-section calculations are not valid approximations [26] and cannot correctly explain the IR absorption bands.

4.3. $MgAl_2O_4$

Group-theoretical analysis [40, 41] predicts for materials with the spinel structure ($Fd\bar{3}m$)

four IR-active modes, so we began by using a classical four-phonon model to fit the experimental reflectance of the pellet. However, we could not reach a satisfactory fit. More recently Striefler and Boldish [42] fitted the single-crystal reflectance spectrum using a six-oscillator model; these authors justified the two additional oscillators because MgAl_2O_4 suffers a small distortion that breaks the $Fd\bar{3}m$ symmetry of spinels down to $F\bar{4}3m$ [43, 44], and in this space group the structure will have seven IR-active bands. These irregularities have also been detected in the powder reflectance spectrum, so we finally used a six-oscillator model as well. The final adjustment is shown in figure 4 and in table 3, where our results are compared to the published single-crystal parameters [42]. The resonance frequencies of the main modes calculated from the powder spectra agree reasonably well (within 10%) with those obtained from a single crystal, and the same can be said of the strength and damping parameters. The exception is the powder mode placed at 414 cm^{-1} , which corresponds to the mode at 363 cm^{-1} in the single crystal. This mode is strongly active and its value for the strength deviates considerably from the value obtained in the crystal, but this oscillator is strongly damped ($\gamma = 115$), so that its relative importance could be equivalent to that of the 363 cm^{-1} single-crystal mode. In the case of the powder modes at 628 and 663 cm^{-1} , it seems that they represent a splitting of the 674 cm^{-1} single-crystal mode, attributable to an artifact of the least-squares procedure; if this is so, then the weak single-crystal mode at 581 cm^{-1} goes undetected.

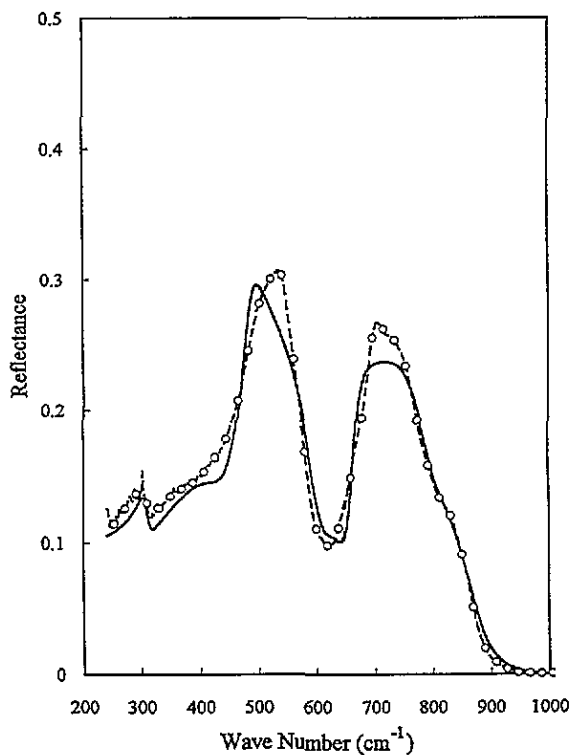


Figure 4. The IR reflectance spectrum of powdered spinel, MgAl_2O_4 : (---O---) measured values; (—) values calculated using the PPP parameters in table 3.

Table 3. The IR optical parameters of MgAl_2O_4 from pressed powder pellet ($f = 0.48$, $\epsilon_\infty = 2.96$ [42], fixed; $f_c = 0.54$, refined) obtained in this paper (PPP) by least-squares fit ($\mathcal{R} = 0.09$), and single-crystal (sc) parameters published by Striefler *et al* [42].

ω_T (cm^{-1})		$4\pi\rho$		γ (cm^{-1})	
PPP	SC	PPP	SC	PPP	SC
307 ± 2	306	0.37 ± 0.09	0.334	19 ± 6	19
414 ± 6	363	2.8 ± 0.34	0.145	115 ± 15	49
484 ± 1	491	3.1 ± 0.16	3.526	27 ± 2	32
628 ± 5	581	0.30 ± 0.07	0.022	70 ± 10	23
663 ± 1	674	0.32 ± 0.04	0.714	26 ± 3	29
811 ± 6	812	0.010 ± 0.001	0.015	60 ± 20	52

4.4. CaF_2

The IR dielectric constants of fluorite were reported by Kaiser *et al* [45]. The material features a main IR mode, in agreement with group-theoretical prediction, and a small additional mode that can be attributed to an interaction between an optical and an acoustic phonon. The experimental powder reflectance spectra and the best fit we get appear in figure 5. In this case we have measured a very high value of the filling factor ($f = 0.75$), which can be due to the high plasticity that is characteristic of halides. A comparison between powder and single-crystal oscillator parameters, table 4, reveals a small disagreement (within 10%) in the frequency of the second oscillator. Since its reflection band is located in the middle of the wide plateau of the main mode, it turns out to be rather difficult to detect. Another disagreement is found in the larger value of the damping parameter of the main oscillator as obtained from powder data, which is 2.7 times greater than the corresponding single-crystal value. In this case we think this high damping value is a consequence of the large value of the filling factor of the pellet. At this compaction ratio the original individual powder particles are partially sintered (figure 1(e)), with the consequence that the concepts of particle shape, and indeed even of individual particles, lose their original sense, and equation (2) no longer provides an accurate representation of the system. Furthermore in this case we have found a strong correlation between damping, filling factor and percolation threshold in the *reststrahl* region.

Table 4. The IR optical parameters of CaF_2 from pressed powder pellet ($f = 0.75$, $\epsilon_\infty = 2.045$ [45], fixed; $f_c = 0.6$, refined) obtained in this paper (PPP) by least-squares fit ($\mathcal{R} = 0.04$), and single-crystal (sc) parameters published by Kaiser *et al* [45].

ω_T (cm^{-1})		$4\pi\rho$		γ (cm^{-1})	
PPP	SC	PPP	SC	PPP	SC
264.1 ± 0.3	257	3.90 ± 0.03	4.2	12.4 ± 0.5	4.63
359 ± 2	328	0.38 ± 0.02	0.40	130 ± 4	115

4.5. SrTiO_3

The crystal structure at room temperature of this compound belongs to the ideal perovskite type, space group $Pm\bar{3}m$, and it has been chosen in this study because of its high dielectric constant at low frequency.

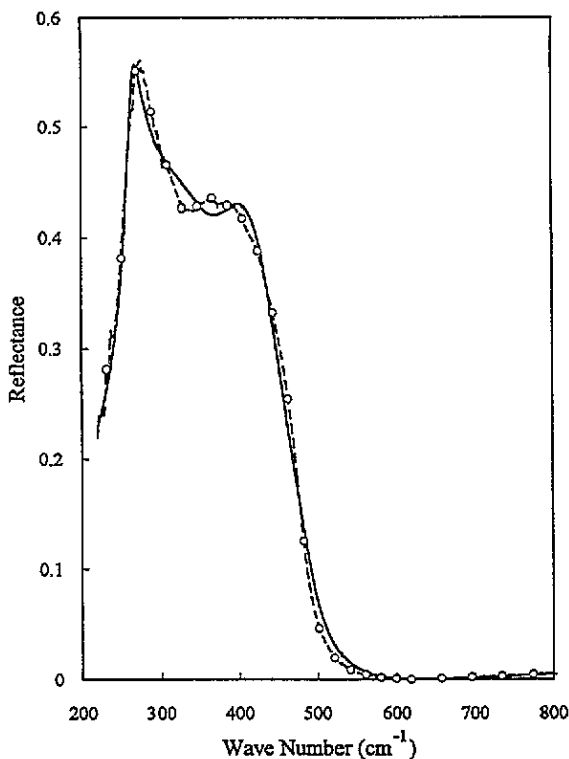


Figure 5. The IR reflectance spectrum of powdered CaF_2 : (---○---) measured values; (—) values calculated using the PPP parameters in table 4.

The IR dielectric constant for SrTiO_3 was first measured on single-crystal material by Spitzer *et al* [46], who used a classical harmonic three-oscillator model, following the predictions of group theory. However, the final fit achieved by these authors was not satisfactory. Later, Barker and Hopfield [47] tried to fit the single-crystal reflectance spectrum with a model of coupled oscillators, for which it was necessary to include an additional set of parameters to describe the coupling between modes. In this case a good fit was achieved, but at the cost of using a phenomenological model. Finally, Servoin *et al* [48] used a semi-quantum expression as a model of the dielectric constant (see equation (11) above). Application of this scheme showed that the origin of the disagreement between the data and the predictions of the classical model is the implicit supposition that the damping constant is the same for the longitudinal and transverse optical phonons. In SrTiO_3 the $\omega_L - \omega_T$ splitting is very important (around 300 cm^{-1} for the 175 cm^{-1} oscillator) and the value of the damping at ω_T and ω_L should be different, a fact that is taken into account in equation (11). This model has been employed in materials where the classical model does not work properly [30, 49]. Using this model, Servoin [48] was able to study the temperature variation of the dielectric constant of SrTiO_3 from single-crystal reflectance data.

Some preliminary tests performed with classical oscillators turned out to be unsuccessful for our powder data as well, so we finally decided to use the more recent semi-quantum model (equation (11)) to fit the SrTiO_3 reflectance spectra. The experimental powder reflectance spectrum and our best fit, obtained with three different oscillators, are shown in

Table 5. The IR optical parameters of SrTiO₃ from pressed powder pellet ($f = 0.75$, $\epsilon_{\infty} = 5.2$ [48], fixed; $f_c = 0.55$ refined) obtained in this paper (PPP) by least-squares fit ($\mathcal{R} = 0.06$), in comparison with single-crystal (sc) parameters published by Servoin *et al* [48].

ω_T (cm ⁻¹)		γ_T (cm ⁻¹)		ω_L (cm ⁻¹)		γ_L (cm ⁻¹)	
PPP	SC	PPP	SC	PPP	SC	PPP	SC
103 ± 2	89	100 ± 3	25	177 ± 1	172	9 ± 2	4
179 ± 2	175	11 ± 2	6	473.2 ± 0.5	475	15 ± 1	5
548 ± 1	544	20 ± 1	17	790 ± 1	798	89 ± 3	26

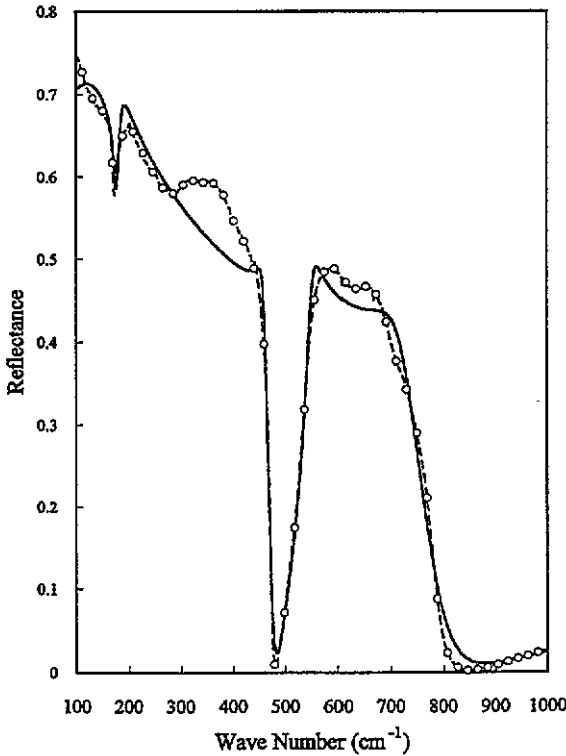


Figure 6. The IR reflectance spectrum of powdered SrTiO₃: (---○---) observed values; (—) values calculated using the PPP parameters in table 5.

figure 6. In these conditions, an acceptable degree of agreement has been obtained. Looking at the results (table 5), we can observe how, in general, the powder frequencies we get are similar to those from the single crystal. The transverse damping parameters of the first and second oscillators are larger than their single-crystal counterparts. We think that these strong modes are affected by sample crystallinity; in this case, the spherical particles obtained by spray pyrolysis are originally amorphous, and develop crystal order through annealing, so it is reasonable to expect a degree of order not as good as that in a single crystal. It must also be pointed out that the damping parameters of the longitudinal modes are of the order of three times as big as those found in the single crystal. The origin of this could be sought not only in the low crystallinity of the sample but mainly in the discontinuity in the reflectance expression when $|\epsilon| \simeq 0$ near to ω_L . In this spectral region, $R(\epsilon) \rightarrow 0$ as $\epsilon \rightarrow 0$ in the

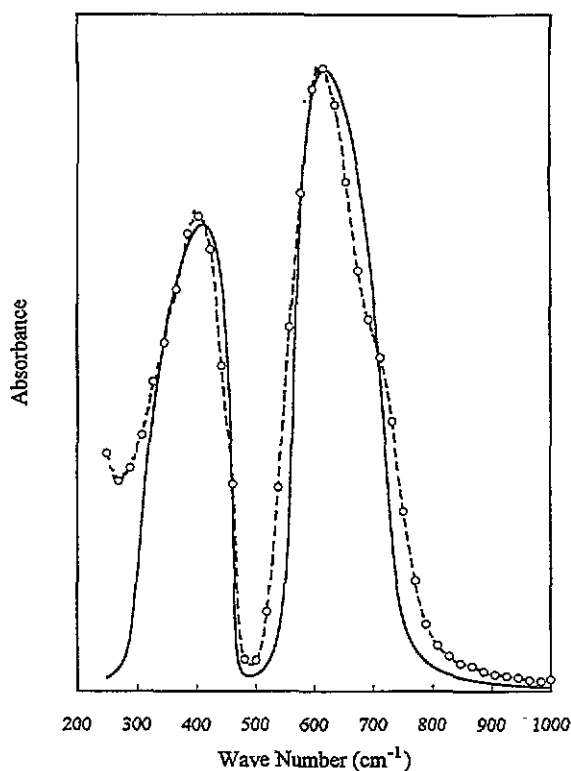


Figure 7. The IR absorbance spectrum of SrTiO_3 particles diluted in KBr ($\epsilon_m = 2.35$): (---○---) observed function; (—) calculated values ($f = 0.10$, $f_c = 0.45$, optical parameters from [48]).

quadrant $\text{Re}(\epsilon) > 0$, while $R(\epsilon) \rightarrow 1$ as $\epsilon \rightarrow 0$ in the quadrant $\text{Re}(\epsilon) < 0$. As a result of this, any small error in the average dielectric constant as computed by equation (2) is amplified by the behaviour of the reflectance expression in the neighbourhood of $|\epsilon| \simeq 0$. This fact must generally occur in all our computed spectra, and becomes more conspicuous when the transverse and longitudinal damping parameters are separately considered.

Another problem is posed by the wide maxima observed at 300–450 and 650–700 cm^{-1} , near the ω_L frequencies (figure 6). It seems that the origin of these features lies in the very nature of the powdered sample and that these maxima, observed between ω_T and ω_L in all the compounds studied, do not correspond to any additional vibrational modes. In this sample, the misfit in these spectral regions could also be due to some degree of particle sintering in the pellet surface, as can be observed in figure 1(h). However, in this case, IR transmission experiments (figure 7) also suggest that there could be some differences between single-crystal and powder dielectric constants that could cause the small shoulders located at 475 and 720 cm^{-1} in this transmission spectrum.

It should be noted that our measurements stop at around 100 cm^{-1} . We know that the lowest-frequency oscillator of this material is in the vicinity of 90 cm^{-1} , so this band has not been accurately fitted.

4.6. Discussion

In general, we can conclude that the use of equation (2) to fit reflectance spectra from powder

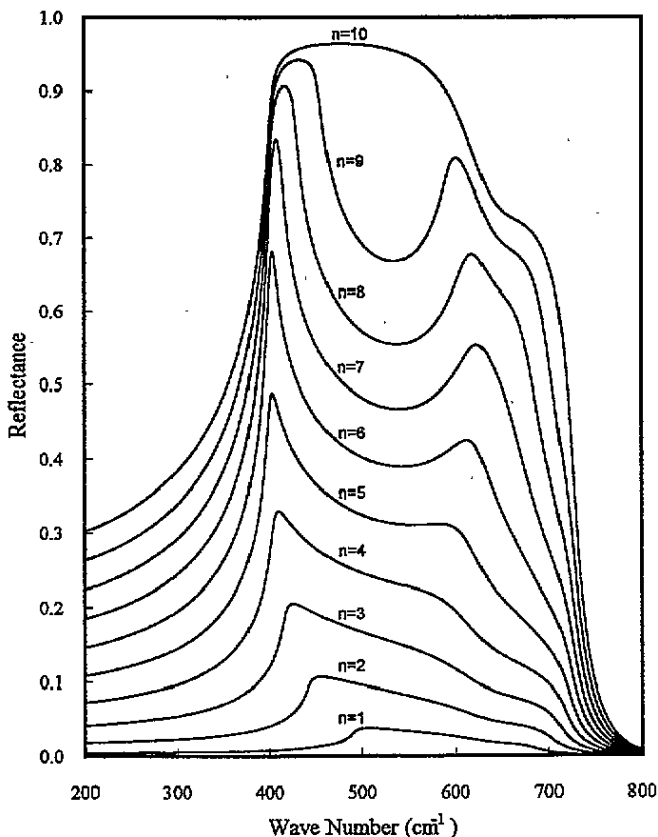


Figure 8. The IR reflectance spectrum of MgO, calculated for $f_c = 0.5$, $f = n\Delta f$, $\Delta f = 0.1$, where n is an integer running from 1 to 10.

pellets is an effective method to obtain experimentally dielectric constants from powdered samples in the infrared. The results are very similar to those obtained from single crystals. The frequencies ω_T and ω_L of the normal modes as determined from powdered samples are similar to those from single crystals. However, there exist, in some cases, discrepancies in the values of the damping parameters. In general we may conclude that this does reflect a real difference between the damping factors in powder and in the single crystal, the former being at most 2–3 times the latter, but normally not much more than this. In the case of SrTiO_3 we attribute the observed disagreement to two additional circumstances: the high value of the single-crystal dielectric constant and the large filling factor of the pressed pellets. If the modulus of the dielectric constant of an ionic substance is very large near ω_T and very small near ω_L , the EMT approximation could lose accuracy in a range of frequencies near ω_L . If the density of the pellet is high there exist some difficulties in the definition of individual particles (see figures 1(c), (e), (h), and microparticle shape variation or even retardation effects cannot be ruled out. Finally, we think that in some cases, such as SrTiO_3 , it could be possible that a difference in the dielectric constant between a single-crystal and microparticles can exist, especially when the crystallinity of the powder particles is not very high.

A difficulty of the method presented here is the high correlation dependences between f , f_c , ϵ_∞ and γ_k . We have found that the best available experimental estimates of f

and ϵ_∞ must be used, and then the refinement of the other parameters can be attempted. We have also detected some complications when two IR modes very close in frequency are present. In this case the correct determination of the optical parameters of each mode becomes difficult, since these will be strongly correlated.

In the best working conditions (small spheroidal particles, $f < 0.6$ and $|\epsilon(\omega)| < 10^2$), i.e. when the EMT hypotheses are fulfilled, the agreement between powder and single-crystal dielectric constants and optical parameters is remarkably good as we have shown in the cases of NiO and MgAl_2O_4 . These conditions can be acceptably satisfied in many metal oxides and practically all covalent substances.

Finally, we want to point out the importance of using an adequate expression for EMT. We have found how equation (2) correctly reproduces the shape of the experimental reflectance band. For a strong IR mode in an ionic compound, a given single-crystal reflectance band that extends with maximum reflectance from ω_T to ω_L transforms in the powder case to a sharp maximum at ω_T , followed by a shallow minimum and a wide plateau, which extends to near ω_L . This implies a non-linear variation of reflectance with filling factor. We have observed this behaviour in all the compounds studied, partially in MgAl_2O_4 and NiO and clearly in MgO, CaF_2 and SrTiO_3 . We have also confirmed that equation (2) reproduces these features approximately, as can be seen in figure 8, where the calculated spectra of aggregates of MgO are plotted for different filling factors (in this case we have used the single-crystal parameters for the dielectric constant that appear in table 2). It is not easy to obtain an analytic expression to determine the position of the reflectance minimum and maximum of the spectrum of the aggregate. We have observed that these frequencies are mainly affected by f . The parameters r and f_c do not notably modify the position of the maximum and minimum, especially in the range $0.4 < f < 0.8$, but they do modify the value of the reflectance.

Acknowledgments

The authors wish to extend their thanks to Dr T González-Carreño, who provided all the samples, and prepared some of them to specifications for this work. Her expertise and kindness are gratefully acknowledged.

References

- [1] Kittel C 1981 *Introducción a la Física del Estado Sólido* (Barcelona: Reverté)
- [2] Palik E D (ed) 1985 *Handbook of Optical Constants of Solids* (Orlando, FL: Academic)
- [3] Born M and Huang K 1964 *Dynamical Theory of Crystal Lattices* (London: Oxford University Press)
- [4] Volz F E 1983 *Appl. Opt.* **22** 1842
- [5] Bliss M, Walden B L and White W B 1990 *J. Am. Ceram. Soc.* **73** 1078
- [6] Shirai H, Morioka Y and Nakagawa I 1982 *J. Phys. Soc. Japan* **51** 592
- [7] Lutz H D, Müller B and Steiner H J 1991 *J. Solid State Chem.* **90** 54
- [8] Bohren C F and Huffman D R 1983 *Absorption and Scattering of Light by Small Particles* (New York: Wiley) p 282
- [9] Van Beek L K H 1967 *Progress in Dielectrics* vol 7, ed J B Birks (London: Heywood) p 69
- [10] Garland J C and Tanner D B (ed) 1978 *Electrical Transport and Optical Properties of Inhomogeneous Media, Proc. 1st Conf. on Electrical Transport and Optical Properties of Inhomogeneous Media (AIP Conf. Proc. 40)* (New York: American Institute of Physics)
- [11] Lafait J and Tanner D B (ed) 1989 *Proc. 2nd Int. Conf. on Electrical Transport and Optical Properties of Inhomogeneous Media; Physica A* **157** No 1
- [12] Maxwell-Garnett J C 1904 *Phil. Trans. R. Soc.* **203** 385; 1905 *Phil. Trans. R. Soc.* **205** 237

- [13] Bruggerman D A G 1935 *Ann. Phys. Lpz.* **24** 636
- [14] Landauer R 1952 *J. Appl. Phys.* **23** 770
- [15] Landauer R 1978 *Electrical Transport and Optical Properties of Inhomogeneous Media, Proc. 1st Conf. on Electrical Transport and Optical Properties of Inhomogeneous Media (AIP Conf. Proc. 40)* ed J C Garland and D B Tanner (New York: American Institute of Physics) p 2
- [16] Genzel L and Martin T P 1972 *Phys. Status Solidi* **b** **51** 91
- [17] Hayashi S, Nakamori N and Kanamori H 1979 *J. Phys. Soc. Japan* **46** 176
- [18] Serna C J, Ocaña M and Iglesias J E 1987 *J. Phys. C: Solid State Phys.* **20** 473
- [19] Iglesias J E, Ocaña M and Serna C J 1990 *Appl. Spectrosc.* **44** 418
- [20] Ocaña M and Serna C J 1991 *Spectrochim. Acta* **47A** 765
- [21] Pecharrmán C, González-Carreño T and Iglesias J E 1993 *Appl. Spectrosc.* **47** 1203
- [22] Hashin Z and Strikman S 1962 *J. Appl. Phys.* **33** 3125
- [23] Bergman D J 1978 *Electrical Transport and Optical Properties of Inhomogeneous Media, Proc. 1st Conf. on Electrical Transport and Optical Properties of Inhomogeneous Media (AIP Conf. Proc. 40)* ed J C Garland and D B Tanner (New York: American Institute of Physics) p 46
- [24] Bergman D J 1982 *Ann. Phys., NY* **138** 78
- [25] Gosh K and Fuchs R 1991 *Phys. Rev. B* **44** 7330
- [26] Pecharrmán C and Iglesias J E 1994 *Phys. Rev. B* **49** 7137
- [27] González-Carreño T, Mifsud A, Serna C J and Palacios J M 1991 *Mater. Chem. Phys.* **27** 287
- [28] Porteus J O 1963 *J. Opt. Soc. Am.* **53** 1394
- [29] Beckmann P and Spizzichino A 1987 *The Scattering of Electromagnetic Waves from Rough Surfaces* (Norwood, MA: Artec House) ch 5
- [30] Gervais F and Pirou B 1974 *Phys. Rev. B* **10** 1642
- [31] Gervais F and Pirou B 1974 *J. Phys. C: Solid State Phys.* **7** 2374
- [32] Cohen R W, Cody G D, Coutts M D and Abeles B 1973 *Phys. Rev. B* **8** 3689
- [33] Gielisse P J, Plendl J N, Mansur L C, Marshall R, Mitra S S, Mykolajewycz R and Smakula A 1965 *J. Appl. Phys.* **36** 2446
- [34] Mochizuki S and Satoh M 1981 *Phys. Status Solidi* **b** **106** 667
- [35] Jasperse J R, Kahan A, Plendl J M and Mitra S S 1966 *Phys. Rev.* **146** 526
- [36] Luxon J T, Montgomery D J and Summit R 1969 *Phys. Rev.* **188** 1345
- [37] Fuchs R 1975 *Phys. Rev. B* **11** 1732
- [38] Tong S Y and Maradudin A A 1969 *Phys. Rev.* **181** 1318
- [39] Genzel L and Martin T P 1972 *Phys. Status Solidi* **b** **51** 101
- [40] Waldron R D 1955 *Phys. Rev.* **99** 1727
- [41] White W B and DeAngelis B A 1967 *Spectrochim. Acta* **23A** 985
- [42] Striefler M E and Boldish S I 1978 *J. Phys. C: Solid State Phys.* **11** L237
- [43] Grimes N W 1972 *Phil. Mag.* **26** 1217; 1972 *Spectrochim. Acta* **23A** 2217
- [44] Mishra R K and Thomas G 1977 *Acta Crystallogr. A* **33** 678
- [45] Kaiser W, Spitzer W G, Kaiser R H and Howarth L E 1962 *Phys. Rev.* **127** 1950
- [46] Spitzer W G, Miller R C, Kleinmann D A and Howarth L E 1962 *Phys. Rev.* **126** 1710
- [47] Barker A S and Hopfield J J 1964 *Phys. Rev.* **135** A1732
- [48] Servoin J L, Luspín Y and Gervais F 1980 *Phys. Rev. B* **22** 5501
- [49] Gervais F, Pirou B and Cabannes F 1973 *J. Phys. Chem. Solids* **34** 1785